Available online at www.sciencedirect.com
ScienceDirect
European Polymer Journal 43 (2007) 2956–2966
EUROPEAN POLYMER JOURNAL
www.elsevier.com/locate/europolj

Biopolymeric delivery system for controlled release of polyphenolic antioxidants

Liyan Zhang, Shantha L. Kosaraju *

Food Science Australia, Victoria-3030, Australia

Received 23 February 2007; received in revised form 19 April 2007; accepted 19 April 2007
Available online 6 May 2007

Abstract

A chitosan based delivery system has been developed for the controlled release of polyphenolic antioxidants such as catechin. Placebo and catechin entrapped particulate delivery systems were prepared using the sodium tripolyphosphate ionic crosslinking technique. The particles have been characterised by transmission electron microscopy, particle size and charge distribution analysis, Fourier Transform infrared spectroscopy, differential scanning calorimetry and entrapment efficiency studies. These studies gave an understanding of the physico-chemical interactions that influence the biopolymer during particle formation and entrapment of catechin. The *in vitro* release of catechin was carried out in enzyme-free simulated gastric and intestinal fluids. Although nanoparticles could be formed by the crosslinking technique used, there was aggregation behaviour observed after retrieval and freeze-drying of the particles as shown by transmission electron microscopy. Both the placebo and catechin-loaded particles had mean particle size range of about 4.27–6.29 μm after freeze-drying and were charged. Fourier Transform infrared spectroscopy, differential scanning calorimetry studies indicated minor structural interactions between catechin and chitosan matrix. Entrapment efficiency of the particles ranged between 27% and 40%. *In vitro* release studies indicated that the release of catechin in simulated gastric and intestinal fluids was between 15% and 40%, depending on the structural interactions between catechin and the chitosan matrix.

Keywords: Chitosan; Particles; Entrapment; Catechin; Controlled release

1. Introduction

Phenolic compounds have over 8000 various structures but the main feature is one aryl ring with a hydroxyl group on it [1]. The major sources of polyphenolic compounds in diet are found in fruits and beverages, especially in tea and coffee [2]. Among these polyphenolic compounds, catechin which is a flavonoid, creates a centre of consideration due to its noticeable antioxidant activity. Numerous studies have proven that catechin has various types of pharmacological properties including anti-oxidative, anti-inflammatory, anti-mutagenic, anti-carcinogenic, antiangiogenic, apoptotic, anti-obesity, hypocholesterolemic, anti-arteriosclerotic, anti-diabetic, anti-bacterial, anti-viral, and anti-aging effects [3]. On the other hand, some studies showed that the antioxidant activity of catechin decreased dramatically when it is exposed to

* Corresponding author. Fax: +61 3 9731 3250.
E-mail address: shantha.kosaraju@csiro.au (S.L. Kosaraju).

0014-3057/$ - see front matter
doi:10.1016/j.eurpolymj.2007.04.033

alkaline pH as in the human intestine. Record and Lane in 2001 [4] have demonstrated that the incubation of green and black tea at alkaline pH could cause rapid decline of concentration of catechin, but with a lesser reduction in antioxidant activity and polyphenol concentration. This is probably due to the formation of dimers as suggested by Yoshino et al. [5]

The function and concentration of catechin in human plasma after ingestion has also been studied. It was concluded by Nakagawa et al. in 1999 that catechin-incorporated plasma is highly resistant to Cu^{2+}-dependant *in vitro* lipid peroxidation. This denoted that ingestion of catechin helps to increase the antioxidant capacity of human plasma, thereby reducing the risk of cardiovascular disease by preventing oxidative modification of plasma lipoproteins. However, the decrease in concentration of catechin was moderately rapid in the plasma [6].

With the objective of protecting catechin in intestinal conditions and also to increase the plasma concentration levels of catechin by controlled/sustained release, an entrapment technique was utilized in this investigation. Catechin was encapsulated using chitosan. Chitosan is a biomaterial which is both biodegradable and biocompatible. It is a cationic polysaccharide and is next to cellulose in abundance in nature. It is being chosen as a drug delivery system in the treatment of various diseases due to its biocompatible and mucoadhesive properties [7]. Furthermore, chitosan can also induce sustained release of the encapsulated bioactive due to its mucoadhesive property. This helps in increasing the transport of molecules across mucosal barriers [8]. However, chitosan is only soluble in acidic environment which decreases the availability of bioactive in the small-intestine. Therefore, many studies have been directed towards modified chitosan to overcome this negative aspect and release of the bioactive in the small-intestine. Xu and Du [9], Hong et al. [10] have prepared chitosan nanoparticles based on chitosan and tripolyphosphate. They treated bovine serum albumin (BSA) as a model protein entrapped into the particles and altered different factors such as temperature, pH, ratio of chitosan to tripolyphosphate, concentration of BSA and molecular weight of chitosan to enhance the entrapment efficiency and release profiles.

While chitosan has been extensively exploited as an encapsulant material for drug entrapment, there appears to be no previous study on catechin as bioactive. Studies intended to complex polysaccharides such as chitosan with polyphenols in order to attain the release of polyphenols *in vivo* found that the process might be reversible [10,11].

Considering the function in metabolic processes as well as properties of polyphenols manifested *in vitro*, entrapment using chitosan is expected to protect catechin from interactions with the food matrix and also to allow controlled release in the gastrointestinal tract. Hence in the current study, chitosan is used as an encapsulant material for entrapment of catechin. Both catechin loaded and un-loaded particles were prepared with the inter and intra-molecular ionic crosslinking of the amino groups of chitosan and phosphate groups of sodium tripolyphosphate (STP). Both the placebo and catechin entrapped particles were characterized by, particle size distribution analysis, zeta potential measurements, Fourier Transform infrared spectroscopy (FTIR), differential scanning calorimetry (DSC) and entrapment efficiency studies. The *in vitro* release of catechin was carried out in simulated gastric and intestinal fluids (SGF and SIF).

2. Experimental

2.1. Materials

Chitosan (molecular weight, 630 kDa) with 90% degree of deacetylation was obtained from Swift chemical company, Australia. STP (NaP_3O_{10}) was from AJAX Chemicals, Sydney, Australia. Catechin [(2R, 3S)-2-(3,4-dihydroxyphenyl)-3,4-dihydro-1 (2H)-benzopyran-3,5,7-triol (+)-catechin hydrate, (minimum 98% by TLC)] was purchased from Sigma–Aldrich, Australia. Folin-Ciocalteu's reagent (2 M) was from Sigma–Aldrich, Australia. All other reagents were of analytical grade and used as received.

2.2. Methods

2.2.1. Particle formation

2.2.1.1. Placebo chitosan particles. 1% (w/w) chitosan solution was prepared using aqueous acetic acid (2% v/v) and the pH was adjusted to 4.7 with 1 M sodium hydroxide. STP (0.5% w/v) solution was added dropwise to the chitosan solution in a fixed weight ratio of chitosan:STP (2.5:1, 5:1, 7.5:1 and 10:1). Chitosan particles were formed spontaneously when adding STP solution to the chitosan solution while stirring. Particles were separated by centrifugation using Beckman Model J2-MC centrifuge at 9820*g* for 30 min. The supernatant was

stored for further analysis. Chitosan particles were rinsed with distilled water and centrifuged under the same conditions. The particles were then freeze-dried by Dynavac FD-5 freeze drier (−40 °C) for around 24 h and stored at 4 °C.

2.2.1.2. Preparation of catechin loaded chitosan particles. An appropriate amount of catechin (10% w/w of chitosan) dissolved in absolute ethanol (0.5–0.8% v/v of chitosan solution) was added to the chitosan solution and followed the same procedure as for the preparation of placebo particles.

2.2.2. Characterisation

Particle size distribution was studied by Malvern Zeta Sizer Nano Series, Nano-ZS. Transmission electron microscopy of chitosan and catechin-loaded chitosan particles was carried out by placing the microspheres in an aqueous medium and ultransonicating for 5 min to produce a suspension. A drop of the suspension was placed on a #200 mesh copper grid which was coated with a carbon coated Formvar film and allowed to evaporate in air. Once evaporated the samples were placed in a JEOL 2010 TEM for imaging. The accelerating voltage used was 100 kV and the images were taken on a Gatan electron energy loss spectrometry (EELS) system using a 6 eV energy slit.

Zeta potential measurements of the particles were done using the auto titrator connected to the Nano-ZS. FTIR was carried out by the potassium bromide pellet method on Excalibur Series FTS 3500GX in the 500–4000 cm^{-1} range. DSC was carried out by Perkin–Elmer Pyris Series DSC 7 with an initial purge of nitrogen at a heating rate of 5 °C min^{-1}.

2.2.2.1. Entrapment efficiency. Entrapment efficiency was calculated using the formula given below.

$$\%\ \text{Entrapment efficiency} = \frac{\text{Total amount of catechin taken for entrapment} - \text{amount of catechin in the supernatant}}{\text{Total amount of catechin taken for entrapment}} \times 100$$

The entrapment efficiency was calculated by estimating the un-entrapped catechin by the total phenolics assay using the Folin-Ciocalteu method [12]. The un-entrapped catechin in the supernatant of each loaded sample was assayed in triplicate and results presented as mean ± SD of three independent experiments.

2.2.2.2. In vitro release. Enzyme free SGF and SIF were prepared according to the US pharmacopoeia [13] and stored at 4 °C before use. Enzyme-free SGF was prepared by dissolving 1 g of sodium chloride and 3.5 ml of concentrated hydrochloric acid (36%) in deionised water and made up to a volume of 500 ml in a volumetric flask.

For the preparation of enzyme-free SIF, 0.2 M sodium hydroxide was prepared by dissolving 800 mg of sodium hydroxide pellets in deionised water and making the volume up to 100 ml. Potassium dihydrogen phosphate (680 mg) was dissolved in deionised water and the volume was made up to 25 ml. 7.7 ml of 0.2 M sodium hydroxide was added to 25 ml of potassium dihydrogen phosphate solution and mixed. The solution pH was adjusted to 6.8 with 0.2 M sodium hydroxide. The volume was made up to 100 ml with deionised water.

Both the placebo and catechin-loaded chitosan particles were incubated at 37 °C and with continuous shaking at 100 rpm in SGF and SIF separately for 2 and 3 h respectively. These conditions are followed as given in the pharmacopoeia to simulate the stomach and the small-intestine. The samples were filtered using 0.2 μm syringe filter and analysed for catechin by the total phenolics assay. All the release studies were conducted in triplicate and results presented as mean ± SD of three independent experiments.

3. Results and discussion

3.1. Preparation of chitosan particles

The preparation of chitosan particles is based on an ionic gelation technique between positively charged chitosan and negatively charged tripolyphosphate at room temperature [9,14,15]. In the original STP solution, the OH^- ions competed with $P_3O_{10}^{-5}$ ions to react with the protonated amino group of chitosan on the surface of beads as soon as the chitosan droplets come into contact with the STP solution. After the formation of a gelled outer layer, the resistance for the larger $P_3O_{10}^{-5}$ ions to diffuse through the gelled film into the inside matrix was higher than the resistance of OH^- ions to diffuse into the beads, due to the smaller molecu-

lar size of OH^-. So, the gelling mechanism of chitosan beads was mainly dependent on coacervation-phase inversion due to the neutralization of protonated amino groups of chitosan accompanied with low ionic crosslinking. The in-liquid curing mechanism of chitosan beads gelling in STP solution could be easily modified from pH-dependent coacervation to ionic crosslinking reaction by adjusting the pH value of STP solution [16].

There are several advantages of using this method including the use of aqueous solutions, formation of smaller particles, manipulation of particle charge by the variation in pH and the possibility of entrapment of proteins or DNA during particle formation [7]. There are some potential drawbacks in this method such as the relatively weak interactions between chitosan and STP under low and high pH conditions. This may cause disintegration of particles under such conditions.

3.2. Characterization

TEM of the particles has indicated the formation of aggregates of the formed particles. Although the particle size of most of the individual particles was below 100 nm as shown in the micrographs (Figs. 1 and 2), formation of aggregates could not be prevented for both the placebo and catechin-loaded particles after drying. The formation of an aggregate of four distinctive single particles with clear joining boundaries formed alongside the regular geometry of the proximate polyhedron (pentagon and hexagon) shaped particles has been reported. This study also suggests the nucleation through ionic gelation followed by semi-crystal formation and growth. BSA-incorporated particles were found

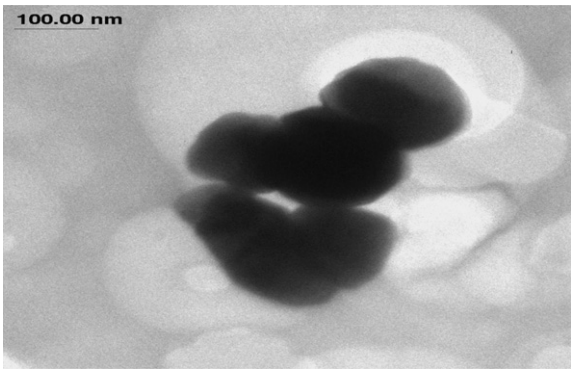

Fig. 1. TEM of chitosan particles prepared using chitosan:STP ratio of 2.5:1.

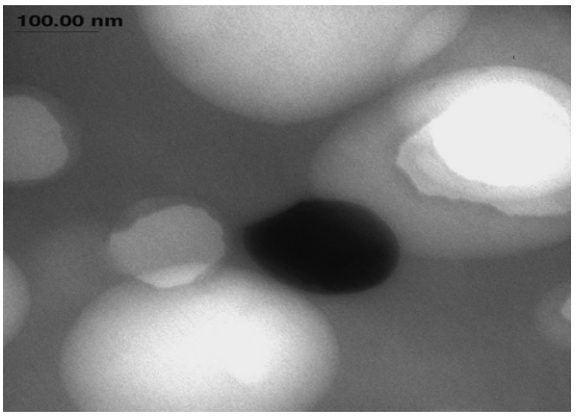

Fig. 2. TEM of catechin-loaded chitosan particles prepared using chitosan:STP ratio of 2.5:1.

to have spherical geometry [17]. However the particle geometry for both placebo and catechin-loaded particles in our studies seemed to be spherical when single particles were observed under TEM. The loss of sphericity on formation of aggregates is also evident in our studies. This may be attributed to the distortion of particle morphology in the aggregated state on drying during sample preparation for TEM studies.

3.2.1. Particle size distribution analysis

Particle size has a crucial impact on the *in vivo* fate of a particulate delivery system and hence control over particle size is of paramount importance [18]. The polydispersity index (PDI) is a measure of dispersion homogeneity and ranges from 0 to 1. Values close to zero indicate a homogeneous dispersion while those greater than 0.3 indicate high heterogeneity. In the previous investigations, chitosan nanoparticles could only be produced in a specific concentration range of chitosan and STP, beyond or below which either aggregation occurred or no particles were formed [7]. Size and size distribution of the chitosan–STP nanoparticles depend largely on concentration, molecular weight, and conditions of mixing, i.e., stirring or sonication. The chitosan–STP nanoparticle colloidal system is thermodynamically unstable, especially at unfavourable solution pH conditions and at high particle concentrations, because of high surface energy associated with the nanoscale dimensions [17]. The mean particle diameter and PDI of both placebo and catechin loaded particles is given in Table 1.

The nanoparticles formed in this study were found to aggregate on drying as evidenced by

Table 1
Zeta-average size and polydispersity index of chitosan particles prepared using different weight ratios of chitosan:STP

Samples	Average (μm)	PDI
Chitosan placebo 2.5/1	5.80 ± 3.7	0.48 ± 0.47
Chitosan placebo 5/1	5.15 ± 3.7	0.77 ± 0.20
Chitosan placebo 7.5/1	6.29 ± 2.5	0.33 ± 0.19
Chitosan placebo 10/1	4.27 ± 2.4	0.62 ± 0.35
Chitosan loaded 2.5/1	4.71 ± 2.3	0.39 ± 0.23
Chitosan loaded 5/1	1.97 ± 1.3	0.31 ± 0.28
Chitosan loaded 7.5/1	4.00 ± 1.9	0.37 ± 0.16
Chitosan loaded 10/1	6.83 ± 4.9	0.23 ± 0.03

TEM. These aggregates could not be completely broken down even after sonication. The size distribution was carried out using these sonicated samples. The *Z*-average size of the placebo chitosan particles ranged between 4.27 and 6.29 μm. There was a reduction in average particle size for the catechin-loaded particles for particles prepared using chitosan:STP ratios from 2.5:1 to 7.5:1 and the particle size was higher than placebo for particles prepared using 10:1 ratio of chitosan:STP. The PDI for catechin-entrapped particles was found to be lower when compared to the placebo chitosan particles for most of the Ch:STP ratios.

The smaller mean diameter of catechin-loaded chitosan particles prepared using 2.5:1–7.5:1 (chitosan:STP) ratio when compared to the corresponding placebo chitosan particles can be attributed to the higher crosslinking density of these particles. This may be explained due to matrix interactions between the chitosan matrix and catechin which enhances the crosslinking density resulting in reduction of particle diameters. These may be hydrophobic interactions mainly and some covalent linkages may also occur. The amino group in chitosan may react with the quinone ring of the oxidised catechin molecule. These physicochemical interactions between protein and polyphenols have been studied extensively [19]. Similar interactions between chitosan and catechin as shown in Fig. 3 may play a major role on the particle properties and will be discussed further based on the FTIR and thermal analysis data obtained. The higher mean diameter of the catechin loaded particles prepared using 10:1 of chitosan:STP may be due to the entrapment of catechin in the inner phase of the polysaccharide matrix without much interaction with the matrix [20]. The placebo particles were found to have much smaller average particle diameter at this ratio which may be due to higher charge density of the particles which results in reduced aggregation effects.

3.2.2. Zeta potential

The zeta potential of placebo and catechin-loaded particles was obtained in order to determine the surface charge. The stability of the particles can be analysed based on the zeta potential [21]. Higher charge density on the particle surface produces repulsive interactions between particles. This leads to more uniform size distribution and also stability of the particles against aggregation effects and also on storage of emulsions.

The average zeta potential of chitosan particles (weight ratio of 2.5:1) was positive (52.75 mV to 0) from pH 3 to 7.37, which indicates that free (non-cross-linked) amino groups remained on the particle surface. In principle, these surface groups have the potential to be used for bioconjugation, to enable targeted drug delivery of the particles [7]. The positively charged amino groups were almost neutralized when the pH is higher than 7.3. The possible explanation could be the lower level of crosslinking of the amino groups in chitosan. The large particle size of the placebo chitosan particles may be due to the smaller number of ionic linkages between chitosan and STP [7].

The positive surface charge of chitosan particles results in higher stability of particles in suspension through the electrostatic repulsion between particles. The positive charge of particles could also lead to the interaction of particles *in vivo* with the cell membrane of bacteria which is negatively charged [22]. Zeta potential of the chitosan particles decreased with the increasing pH value for each sample. The zeta potential of pure chitosan at pH 3.0 was +56.1 mV and at pH 8.0 was +2.61 mV. For chitosan particles, the zeta potential has declined from +52.75 mV at pH 3.0 to −7.75 at pH 8.0. The pK_a for chitosan particles was 7.36. However the pK_a for pure chitosan did not appear in the pH range of 3–8 as shown in Fig. 4.

The auto titration curves indicate the change in zeta potential with changing pH conditions. The lower pK_a of chitosan particles when compared to chitosan can be attributed to the crosslinking reaction between the amino groups of chitosan and STP.

3.2.3. FTIR

The FTIR spectra of placebo and catechin-loaded chitosan particles along with pure chitosan used for their preparation are shown in Fig. 5.

According to Li [23], the peak between 3300 and 3450 cm^{-1} corresponds to stretching vibration of hydroxyl, amino and amide groups in pure chitosan.

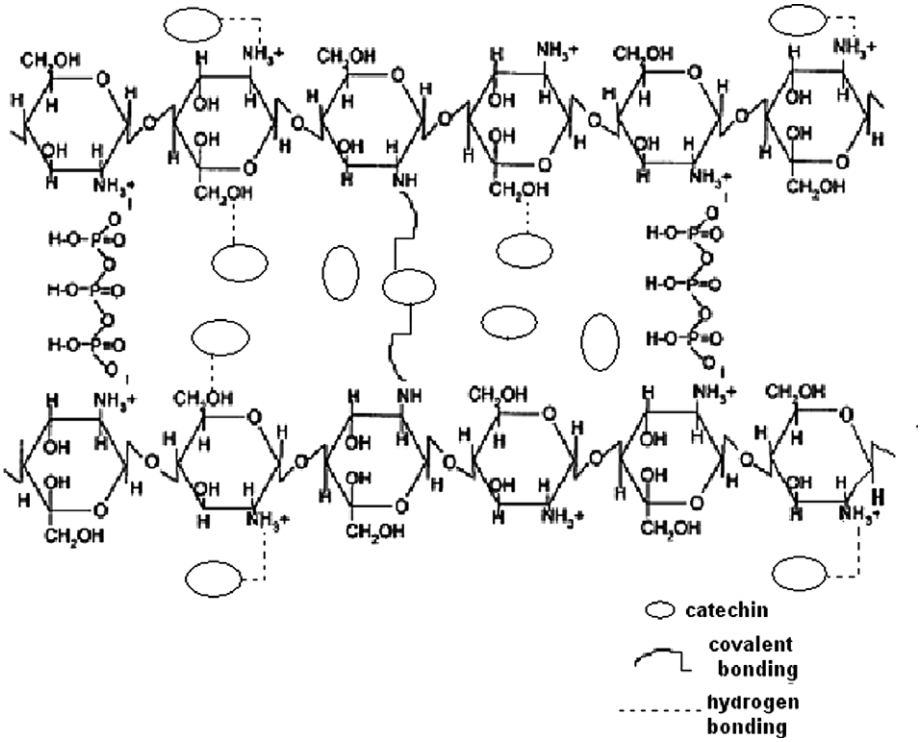

Fig. 3. Physicochemical interaction between chitosan, STP and catechin during particle formation.

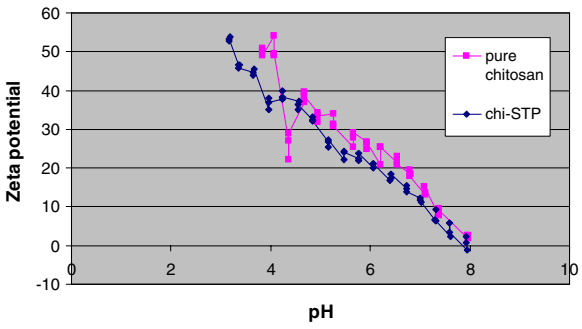

Fig. 4. Autotitration curves for chitosan and chitosan particles.

It is noticeable that this peak has moved to lower wave numbers centered at 3169 cm^{-1} and became broader and stronger in chitosan particles. This indicates the interaction between these groups and sodium tripolyphosphate and also due to hydrogen bonding. Primary amines also show sharp peak between 3500 and 3400 cm^{-1} which could be attributed to the asymmetric and symmetric stretching of the N–H bonds. The peak in pure chitosan and chitosan particles appears broad in this region due to the contribution of O–H stretching peaks and hydrogen bonding [24]. A slight variation of this peak could also be seen after loading catechin. The peak flattened in catechin loaded chitosan particles compared to chitosan particles, which could possibly be due to the interaction of catechin with the un-crosslinked amino groups in chitosan.

Another important change takes place in the range of 1400–1800 cm^{-1}. The shift of 1656 and 1600 cm^{-1} peaks in pure chitosan to 1643 and 1531 cm^{-1} in chitosan particles could be attributed to the linkage between phosphate and ammonium ions, and also reflects that the $–CONH_2$ and $–NH_2$ groups of chitosan are both crosslinked with sodium tripolyphosphate molecule [25,26]. Similar shifts were reported by Xu and Du [9]. The peak for $–NH_2$ bending vibration shifts from 1602 to 1534 cm^{-1}. However for catechin-loaded particles, the peak at 1643 cm^{-1} ($–CONH_2$) changes to 1637 cm^{-1}, peak at 1531 cm^{-1} (N–H bending) remains the same. This indicates minor interactions between hydroxyl groups in catechin and amide group in chitosan crosslinked particles. The new peak at 1208 cm^{-1} indicating P═O stretching [26] appears in un-loaded chitosan particles and disappears in catechin loaded particles, which could be attributed to the change in structure of the matrix after loading catechin.

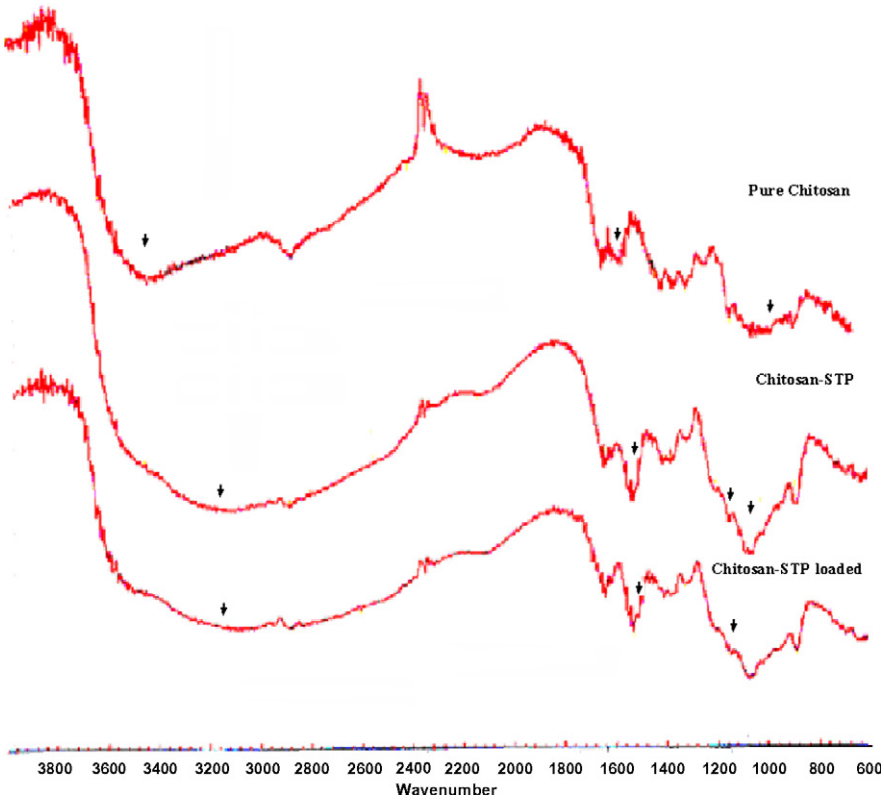

Fig. 5. FTIR of chitosan, chitosan particles and catechin-loaded chitosan particles.

The peak at 1029 cm^{-1} in placebo particles shifted to 1078 cm^{-1} in catechin-loaded particles. This peak is due to the symmetric stretch of C–O–C (around 1020–1075 cm^{-1}) [24]. The interactions between chitosan matrix and catechin has lead to the shift of the peak in catechin-loaded matrix. Therefore, crosslinking between chitosan and STP influences chitosan's conformational structure significantly.

3.2.4. Differential scanning calorimetry

As shown in Fig. 6, the endothermic peak for pure chitosan at 180 °C has shifted to a higher temperature at 194 °C for chitosan particles (chitosan:STP of 2.5). This could be due to the higher crosslinking density of chitosan matrix [27] that the increasing crosslinking could result in a shift of the endothermic peak. The glass transition temperature (T_g) of chitosan depends on a number of factors like crystallinity, molecular weight and degree of deacetylation. These characteristics may vary according to the source and or method of extraction. In the present study we have not observed T_g for chitosan.

For both the placebo and catechin-loaded chitosan particles, two endothermic peaks have been observed. The peaks shift slightly from 194 and 242 °C in placebo to 197 and 238 °C in catechin-loaded particles respectively. Pure catechin shows an endothermic peak at 231 °C. The shift in endothermic peaks of catechin-loaded chitosan particles indicates some minor interaction of catechin and the chitosan matrix. These minor interactions corroborate with the peak shifts as observed in the FTIR spectra.

3.2.5. Entrapment efficiency studies

Entrapment efficiency (EE) of catechin in chitosan particles was estimated by an indirect method in which un-entrapped catechin in the supernatant was estimated. Some of the previous studies also reported this method of estimating entrapment efficiency [9]. This method was chosen due to the difficulty in breaking down the particles or swelling the particles in different media. Similar results were also reported by Shu and Zhu [28]. They examined the electrostatic interactions on the controlled drug release properties of chitosan–phosphates, chitosan–pyrophosphate

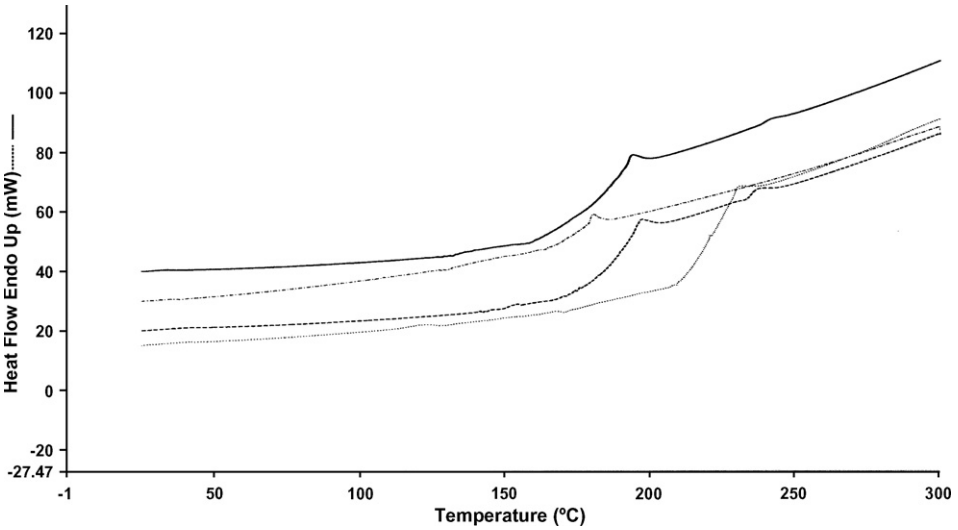

Fig. 6. DSC analysis of chitosan (dash dot); catechin (dot); placebo chitosan particles (solid); catechin-loaded chitosan particles (dash).

and chitosan–tripolyphosphate films. They illustrated that the swelling ratio of chitosan–tripolyphosphate films was much smaller because of the greater charge number of STP and hence the increased ability to crosslink with chitosan. They pointed out that chitosan–STP film could still retain its integrity for more than 48 h even in the media as low as pH 1.5. Based on these previous studies, there is an indication that the catechin entrapped chitosan particles prepared in this study have reinforced crosslinking density due to the structural interactions of catechin and chitosan matrix. Taking into consideration, the result obtained from FTIR and the extremely low swelling of the particles, it is quite possible that the $–CONH_2$ and $–NH_2$ groups in chitosan have interacted with the tripolyphosphate groups in STP through ionic bonding. The interaction between chitosan matrix and catechin in catechin-loaded particles may also contribute to enhanced crosslinking density of the matrix.

From the results shown in Fig. 7, EE of catechin ranged between 27.9% and 40.12%. It was not significantly affected by the weight ratio of chitosan:STP. It can be seen that the entrapment efficiency increased slightly with the increasing weight ratio of chitosan:STP, which could be due to the higher levels of available amino groups in the chitosan. These free amino groups may interact with catechin thus increasing the EE. However there is a considerable decrease of entrapment efficiency at the weight ratio of 10:1. The mean particle size of these particles has increased in this case indicating the reduced interactions between chitosan matrix and catechin. This may be due to the competitive inhibition of crosslinking reactions due to the excessive amino groups being available at higher concentration of chitosan.

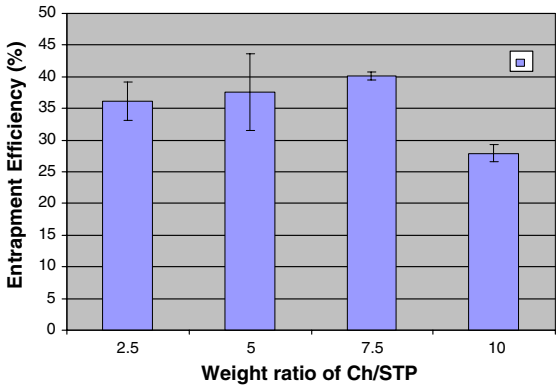

Fig. 7. Entrapment efficiency of chitosan particles.

3.2.6. In vitro release studies

The release profiles of catechin from chitosan particles is shown in Fig. 8. The amount of catechin released based on the total entrapped catechin, ranged between 5% and 15% in SGF and 9% and 25% in SIF, from particles prepared using different weight ratios (2.5:1–10:1) of chitosan to STP.

In SGF, the increasing trend in release may be due to the decreased crosslinking density of the particles. According to Shu and Zhu [28], increasing STP concentration improved the stability of chitosan–STP in SGF due to higher crosslinking density. This could be another reason for the low release

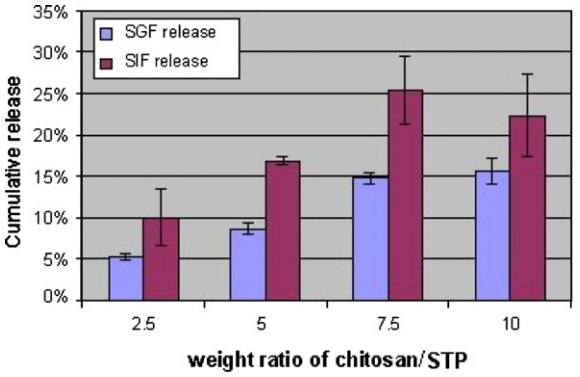

Fig. 8. *In vitro* release of catechin from chitosan particles.

both in SGF and SIF for particles with 2.5:1 ratio. For the ratio 10:1, the release has increased. This might be because for ratio 10:1, the crosslinking is weaker than for ratio 7.5:1, the un-crosslinked amino groups are able to be protonated in acidic conditions. Therefore, the particle swelling will be higher for 10:1 than for ratio 7.5:1. This enhanced swelling will lead to higher release of entrapped catechin

In SIF, there are mainly two possible reasons for the increasing trend in released catechin with the increasing weight ratio of chitosan:STP. The first factor is the entrapment efficiency. If the entrapment efficiency is higher, then accordingly the release will be increased. The second reason is that the crosslinking density of the particles. If the trend of catechin release in SIF is only dependent on entrapment efficiency, such sharp rise in release from the ratio of 2.5–7.5 will not be anticipated. This can be implicated to weaker crosslinking with increasing weight ratio of chitosan:STP. For sample ratio of 10:1, the release is expected to increase slightly because of further reduction in crosslinking density, but the release was found to be lower than for 7.5:1. This may be attributed to the lower entrapment efficiency, which is much lower than the particles prepared with 7.5:1 ratio. As such particles prepared using 10:1 ratio behaved differently as discussed earlier under the PSD analysis when compared to particles prepared with other ratios.

The cumulative release of catechin from particles with 2.5:1, 5:1; 7.5:1 and 10:1 in SGF and SIF amounts to 15.19%, 25.51%, 40.24% and 37.97% respectively. The released amounts were not more than 50%, which means there was still some catechin available for further release. Since chitosan particles are both mucoadhesive and also degradable in the colonic environment, catechin could be further released in large-intestine for prolonged periods.

FTIR analysis indicated that catechin has possible structural interactions with chitosan. This has lead to reduced release. It has been suggested that the interaction of polyphenols with chitosan may be reversible, and at higher pH the release of polyphenols from the complex occurs [11]. This indicates that after the release in stomach and small-intestine, release due to the cleavage between catechin and chitosan may occur in the large-intestine. There may be release of more catechin due to the microbial breakdown of the chitosan matrix.

The major factor to affect the absorption of polyphenol is their ability to interact with dietary or endogenous proteins in the gut [29]. As Piskula and Terao [30] indicated that some of the catechins delivered to the gut can be glucuronidated by the glucuronosyl transferase in the mucosa of the intestine. Consequently, protecting catechin from interaction with these enzymes and also different components of the food matrix in gut is quite important to increase the bioavailability of catechin. From the current *in vitro* study, catechin was well protected (up to 85%) in chitosan particles in SGF for 2 h, and potentially a large percentage of catechin goes down to intestine for absorption.

Yang et al. [31] demonstrated that after absorption, the catechins are widely distributed in all body tissues with the highest concentration found in the oesophagus, intestine and colon. Therefore, the larger the amount of catechin available in the large-intestine, the higher the concentration of catechin in the colon. By increasing the loading concentration of catechin, higher entrapment efficiency may be achieved which in-turn increases the availability of catechin in colon.

4. Conclusion

This present study has investigated the preparation of chitosan based particulate delivery systems for the entrapment and controlled release of catechin. Particle formation was achieved by an ionic gelation technique.

Particles of different size distributions were obtained using different weight ratios of chitosan:STP. Due to the aggregation of the formed nanoparticles as observed by TEM, the average size range varied between 1.97 and 6.83 μm. It was demonstrated that the weight ratio 5:1 has much preferred smaller particle size both in placebo and

catechin-loaded system. The smaller particle size and larger surface area is highly advantageous for tailoring the delivery systems to reach various targeted sites in the body. Chitosan particles characterized by FTIR and DSC confirmed that the particles were formed through crosslinking between positively charged amino groups in chitosan and negatively charged phosphate groups in STP. These studies also indicated that both amido and amino groups ($-CONH_2$ and $-NH_2$) were involved in the crosslinking reaction. In addition, all the particles formed by different ratios of chitosan:STP possess positive zeta potential, which indicates that these particles could be attached to the negatively charged membranes of microorganisms or mucosa in the gastro-intestinal tract to maintain prolonged concentration of catechin *in vivo*.

The entrapment efficiency study suggested that the particles with weight ratio of 7.5:1 (chitosan:STP) have the highest catechin loading capacity. The particles prepared with the weight ratio of 2.5:1 (chitosan:STP) have the highest crosslinking density and the least release both in stomach and small-intestine. Hence there is a great potential for delivery systems with controlled release of catechin in the upper GIT followed by release of the remaining catechin in the large-intestine.

Acknowledgements

The authors acknowledge the financial support from the department of primary industries, Victoria. They would also like to thank Dr. Leif Lundin for many helpful suggestions in preparing this manuscript.

References

[1] O'Connell JE, Fox PF. Significance and applications of phenolic compounds in the production and quality of milk and dairy products: a review. Int Dairy J 2001;11(3):103–20.
[2] Kilmartin PA, Hsu CF. Characterisation of polyphenols in green, oolong, and black teas, and in coffee, using cyclic voltammetry. Food Chem 2003;82(4):501–12.
[3] Koo MW, Cho CH. Pharmacological effects of green tea on the gastrointestinal system. Eur J Pharmacol 2004;500(1–3):177–85.
[4] Record IR, Lane JM. Simulated intestinal digestion of green and black teas. Food Chem 2001;73(4):481–6.
[5] Yoshino K, Suzuki M, Sasaki K, Miyase T, Sano M. Formation of antioxidants from (−)-epigallocatechin gallate in mild alkaline fluids, such as authentic intestinal juice and mouse plasma. J Nutr Biochem 1999;10(4):223–9.
[6] Nakagawa K, Ninomiya M, Okubo T, Aoi No K, Juneja LR, Kim M, et al. Tea catechin supplementation increases antioxidant capacity and prevents phospholipids hydroperoxidation in plasma of humans. J Agric Food Chem 1999;47(10):3967–73.
[7] Hong Z, Megan O, Christine A, Eugenia K. Monodisperse chitosan nanoparticles for mucosal drug delivery. Biomacromolecules 2004;5(6):2461–8.
[8] Thanou M, Verhoef JC, Junginger HE. Oral drug absorption enhancement by chitosan and its derivatives. Adv Drug Deliv Rev 2001;52(2):117–26.
[9] Xu Y, Du Y. Effect of molecular structure of chitosan on protein delivery properties of chitosan nanoparticles. Int J Pharm 2003;250(1):215–26.
[10] Catriona MS, Ya C, Russeli M, Simon HG, Paul NG, Daniele M, et al. Polyphenol complexation – some thoughts and observations. Phytochemistry 1988;27(8):2397–409.
[11] Marcel-Ionel P, Micolae A, Valentin IP, Daniela A. Study of the interactions between polyphenolic compounds and chitosan. React Funct Polym 2000;45(1):35–43.
[12] Singleton VL, Rossi JA. Colorimetry of total phenolics with phosphomolybdic–phosphotungstic acid reagents. Am J Enol Viticult 1965;16(3):144–58.
[13] US Pharmacopia (2000) and National Formulatory (USP 24 NF 19), Rockville (MD).
[14] Calvo P, Remunan-Lopez C, Vila-Jato JL, Alonso MJ. Novel hydrophilic chitosan–poly ethylene oxide nanoparticles as protein carriers. J Appl Polym Sci 1997;63(1):125–32.
[15] De Campos AM, Sanchez A, Alonso MJ. Chitosan nanoparticles: a new vehicle for the improvement of the delivery of drugs to the ocular surface. Int J Pharm 2001;224(1–2):159–68.
[16] Mi FL, Shyu SS, Lee ST, Wong TB. Kinetic study of chitosan–tripolyphosphate complex reaction and acid-resistive properties of the chitosan–tripolyphosphate gel beads prepared by in-liquid curing method. J Polym Sci A2: Polym Phys 1999;37(14):1551–64.
[17] Gan Q, Wang T, Cochrane C, McCarron P. Modulation of surface charge, particle size and morphological properties of chitosan–STP nanoparticles intended for gene delivery. Colloid Surf B: Biointerf 2005;44(2–3):65–73.
[18] Moghimi SM, Hunter AC, Murray JC. Long-circulating and target-specific nanoparticles: theory to practice. Pharmacol Rev 2001;53(2):283–318.
[19] Rohn S, Rawel HM, Kroll J. Antioxidant activity of protein-bound quercetin. J Agric Food Chem 2004;52(15):4725–9.
[20] Jian Du, Sheng Zhang, Rui Sun, Li-Fang Zhang, Cheng-Dong Xiong, Yu-Xing Peng. Novel polyelectrolyte carboxymethyl konjac glucomannan–chitosan for drug delivery. II. Release of albumin *in vitro*. J Biomed Mater Res B: Appl Biomater 2005;72B(2):299–304.
[21] Chansiri G, Lyons RT, Patel MV, Hem SL. Effect of surface charge on the stability of oil/water emulsions during steam sterilization. J Pharm Sci 1999;88(4):454–8.
[22] Lifeng Q, Zirong X, Xia J, Caihong H, Xiangfei Z. Preparation and antibacterial activity of chitosan nanoparticles. Carbohydr Res 2004;339(16):2693–700.
[23] Li Z. Preparation and characterization of CdS quantum dots chitosan biocomposite. React Funct Polym 2003;55(1):35–43.

[24] Banerjee T, Mitra S, Kumar SA, Kumar SR, Maitra A. Preparation, characterization and biodistribution of ultrafine chitosan nanoparticles. Int J Pharm 2002;243(1–2): 93–105.
[25] Wu Y, Yang W, Wang C, Hu J, Fu S. Chitosan nanoparticles as a novel delivery system for ammonium glycyrrhizinate. Int J Pharm 2005;295(1–2):235–45.
[26] Qi L, Xu Z. Lead sorption from aqueous solutions on chitosan nanoparticles. Colloid Surf A: Physicochem Eng Aspect 2004;251(1–3):183–90.
[27] Neto CGT, Giacometti JA, Job AE, Ferreira FC, Fonseca JLC, Pereira MR. Thermal analysis of chitosan based networks. Carbohyd Polym 2005;62(2):97–103.
[28] Shu XZ, Zhu KJ. The influence of multivalent phosphate structure on the properties of ionically cross-linked chitosan films for controlled drug release. Eur J Pharm Biopharm 2002;54(2):235–43.
[29] Carbonaro M, Grant G, Pusztai A. Evaluation of polyphenol bioavailability in rat small intestine. Eur J Nutr 2001;40(2):84–90.
[30] Piskula MK, Terao J. Accumulation of (−)-epicatechin metabolites in rat plasma after oral administration and distribution of conjugation enzymes in rat tissues. J Nutr 1998;128(7):1172–8.
[31] Yang CS, Chung JY, Yang GY, Li C, Meng X, Lee MJ. Mechanisms of inhibition of carcinogenesis by tea. BioFactors 2000;13:73–9.